Preparation and Characterization of Activated Carbon from Eucalyptus Sawdust I. Activated by NaOH

Article *in* Journal of Inorganic and Organometallic Polymers and Materials · September 2013

DOI: 10.1007/s10904-013-9910-1

CITATIONS
17

READS
940

5 authors, including:

Congjin Chen
Guangxi University
41 PUBLICATIONS **623** CITATIONS
SEE PROFILE

Yanmei Huang
Medical University of South Carolina
53 PUBLICATIONS **1,358** CITATIONS
SEE PROFILE

Zhangfa Tong
Guangxi University
402 PUBLICATIONS **6,723** CITATIONS
SEE PROFILE

J Inorg Organomet Polym (2013) 23:1201–1209
DOI 10.1007/s10904-013-9910-1

COMMUNICATION

Preparation and Characterization of Activated Carbon from Eucalyptus Sawdust I. Activated by NaOH

Congjin Chen · Pengcheng Zhao · Yanmei Huang · Zhangfa Tong · Zhixia Li

Received: 24 February 2013 / Accepted: 5 July 2013 / Published online: 17 July 2013

Abstract Eucalyptus sawdust was used as a precursor to prepare activated carbon using NaOH as a chemical activation agent. The effect of preparation conditions on the characteristics of the produced activated carbon used as an adsorbent was investigated. The performance of the activated carbon was characterized by N_2 adsorption–desorption isotherms, Brunauer–Emmett–Teller equation, Barett–Joyner–Halenda equation, scanning electron microscopy and Fourier transform infrared analysis. When the eucalyptus sawdust mass was 30.00 g, with particle sizes between 0.25 and 0.42 mm, and the sawdust was heated and charred before activation by NaOH, the optimized conditions for the preparation of activated carbon was found to be as follows: mass ratio of NaOH to eucalyptus sawdust, 1:2; activation time, 30 min; and activation temperature, 700 °C. The Iodine number and BET surface area of the produced activated carbon was 899 and 1.12×10^3 m^2 g^{-1}, respectively, with a 13.3 % yield. Activated carbon exhibits adsorption isotherms of type IV. The total pore volume, micropore volume and average pore diameter were recorded as 0.636, 0.160 cm^3 g^{-1} and 2.27 nm, respectively. The pore structure of the activated carbon is mainly mesoporous. Carbonyl and hydroxyl groups may also exist on the activated carbon surface.

Keywords Eucalyptus sawdust · Orthogonal test · NaOH activation · Activated carbon · Pore structure

1 Introduction

Activated carbon (AC) is a reproducible and multi-porous adsorbent. It is a carbon-containing substance with developed pore structure, high specific surface area and good adsorption capacity [1]. It also has adsorption, catalysis, thermo-stability and low acid/base reactivity characteristics [2]. Activated carbon is applied in almost all fields [3], and is particularly useful in dealing with pollutants because of its high specific surface area, affluent inner pores and well-developed micropore structure [2–4].

Wood production has significantly increased in China over the last decade. Most of the new wood plantations consist of eucalyptus. Wood processing and appropriate maintenance of forests generates a considerable volume of woody residues, which are partly used as fuel. However, the development of alternative uses for this waste product is important for the Chinese economy. One potential application of wood waste is as a raw material for charcoal and activated carbon production. Charcoal is produced by pyrolysis and has a market as a clean domestic fuel. Activated carbon requires further activation to prepare the solid product resulting from charring. This can be accomplished by chemical activation or partial gasification activation, also called physical activation. Physical activation is a two-step process [5]. The material is carbonized under inert atmosphere and then activated at high temperatures using steam, carbon dioxide or air as the activation reagent

C. Chen (✉) · P. Zhao · Y. Huang · Z. Tong · Z. Li
School of Chemistry and Chemical Engineering, Guangxi University, Nanning 530004, China
e-mail: gxdxccj@163.com; chencongjin@gxu.edu.cn

C. Chen · Z. Tong
Guangxi Key Laboratory of Petrochemical Resource Processing and Process Intensification Technology, Guangxi University, Nanning 530004, China

to produce more porous structures [6]. Chemical activation held in the presence of dehydrating reagents such as KOH [7], K_2CO_3 [8], NaOH [9], $ZnCl_2$ [10], H_3PO_4 [11] and K_2HPO_4 [12], influences the pyrolytic decomposition and inhibits tar formation [13]. These reagents can improve the pore distribution and increase the specific surface area of the carbon-containing adsorbents [14]. The cellulose and lignin content in eucalyptus wood is high, making it a good raw material to produce activated carbon. Activated carbon has previously been prepared from eucalyptus wood chars and activated by CO_2, CO_2-O_2 and steam [15]. To investigate the feasibility of preparing activated carbon from eucalyptus residues by chemical activation, we studied the activation process using NaOH, KOH, $ZnCl_2$ and H_3PO_4.

In this paper, we report the technology for preparing activated carbon from eucalyptus sawdust activated by NaOH via orthogonal experiments. The pore structure parameters of the AC prepared under optimized conditions are determined.

2 Experimental

2.1 Materials, Reagent and Instruments Employed

The Guangxi Gaofeng Farm, China, provided the raw material, *Eucalyptus grandis* sawdust, with particles of 0.25–0.42 mm selected by sieving. Using the standards described for the proximate analysis of solid biofuels GB/T 28731–2012 (China), a proximate analysis of the eucalyptus sawdust was recorded. These results (wt%) indicate that the eucalyptus sawdust is appropriate for use as an industrial raw material, with moisture, ash, volatile matter and fixed carbon contents of 6.88, 0.67, 83.25, and 9.20, respectively.

Sodium hydroxide was used as an activation agent. Aqueous hydrochloric acid (37 %), Iodine, potassium iodide, sodium thiosulfate and the other analytical reagents were used as purchased from the Shanghai Sinopharm Chemical Reagent Company Ltd (Shanghai, China). All chemicals were of analytical grade and made in the Spark Chemical Plant, Pudong New Area, Shanghai.

SX2-4-10 intellective and hyperthermal electric furnace (Shanghai Jia Zhan Instrumentation Equipment Co. Lit,. China), S-3400 scanning electron microscope (S-3400, Japanese Hitachi Corp.), Micromeritics TriStar-3020 adsorption–desorption instrument (American Micromeritics Corp.) and Nicolet 6700 Fourier transform infrared spectrometer (American Nicolet Corp.) were used for the analysis of AC.

2.2 Orthogonal Test Methodology for Optimizing AC Preparation Conditions

From preliminary experimental investigations using NaOH as an activation agent to prepare AC, the weight ratio of NaOH to eucalyptus sawdust, activation time and activation temperature have been noted as the most influential operational parameters [16, 17]. To optimize the preparative conditions, an orthogonal test methodology was used [18, 19]. An L_9 (3^4) orthogonal array with four operational parameters was used to evaluate corresponding optimal values. These parameters, their range and levels are summarized in Table 1. The complete design matrix of the experiments and the results obtained are shown in Table 2.

Table 1 Design factors and levels for AC preparation

Parameters (independent variable)	Symbol	Range and levels		
		1	2	3
NaOH:eucalyptus wood (mass ratio)	A	2:1	3:1	4:1
Activation time (min)	B	30	50	70
Activation temperature (°C)	C	700	800	900

2.3 Preparation of Activated Carbon

Eucalyptus sawdust (30.00 g) with particle size between 0.25 and 0.42 mm was placed in a high temperature tolerant ceramic crucible. The material was heated and carbonized in an electric furnace. The char produced from the carbonization process was ground and mixed with varying amounts of sodium hydroxide pellets (60.00, 90.00, 120.00 g) in a ceramic crucible with a lid, then heated in a furnace pre-heated to a specified temperature (700, 800, 900 °C) and maintained at this temperature for the specified time (30, 50, 70 min). After cooling, the resulting mixture was washed with hot distilled water, a solution of hydrochloric acid (0.10 mol L^{-1}) and hot distilled water to

Table 2 Results of L_9 (3^4) orthogonal array of designed experiments for the preparation of activated carbon

No.	A	B	C	Y_1 (%)	Y_2 ($\times 10^{-2}$ mg g^{-1})	Y_3 ($\times 10^{-2}$ m^2 g^{-1})
1	2:1	30	700	13.3	8.99	11.2
2	2:1	50	800	11.4	5.74	5.81
3	2:1	70	900	9.0	5.50	3.71
4	3:1	30	800	10.5	5.51	5.42
5	3:1	50	900	11.4	5.00	4.39
6	3:1	70	700	13.0	2.87	2.68
7	4:1	30	900	12.4	2.89	3.60
8	4:1	50	700	12.0	3.41	4.13
9	4:1	70	800	10.9	5.15	4.51

A mass ratio of activation agent to eucalyptus sawdust, *B* activation time (min), *C* activation temperature (°C), Y_1 the yield of activated carbon (%), Y_2 iodine number (iodine adsorption capacity of activated carbon) (mg g^{-1}), Y_3 BET surface area of activated carbon (m^2 g^{-1})

Table 3 Analysis of the experimental results of the L_9 (3^4) orthogonal array of prepared activated carbon

Levels	Yield (%)			Iodine number ($\times 10^{-2}$ mg g^{-1})			BET surface area ($\times 10^{-2}$ m^2 g^{-1})		
	A	B	C	A	B	C	A	B	C
k_1	11.2	12.1	12.8	6.74	5.80	5.09	6.91	6.74	6.00
k_2	11.6	11.6	10.9	4.46	4.72	5.47	4.16	4.78	5.25
k_3	11.7	11.0	10.9	3.82	4.51	4.46	4.08	3.63	3.90
R	0.5	1.1	1.8	2.93	1.29	1.00	2.83	3.11	2.10

pH ~7.0. The activated carbon was separated using a filtering method, dried at 110 °C for 24 h and stored in tightly closed bottles until further analysis.

2.4 Characterization of Prepared Activated Carbon

The Iodine number was determined by GB/T12496.8-1999 (China). The yield (Y) of the prepared activated carbon was estimated from the following equation:

$$Y(\%) = Mc/M_0 \times 100$$

where Mc is the weight of the activated carbon and M_0 is the weight of the dried eucalyptus sawdust.

The specific surface area and pore structure of the activated carbon samples were obtained by nitrogen adsorption–desorption isotherm determined at 77.35 K. Prior to testing, the activated carbon was degassed for 2 h at 250 °C under vacuum. The specific surface area, S_{BET}, was determined from the isotherms using the Brunauer–Emmett–Teller (BET) equation at a relative pressure of $P/P_0 = 0.05 - 0.35$. The total pore (less than 284.8 nm in diameter) volume (V), was defined as the volume of liquid nitrogen adsorbed at a relative pressure of $P/P_0 = 0.993$. The micropore volume (V_{micro}), the micropore area (S_{micro}), and the external surface area (S_{exter}) were determined by the t-plot model equation. The pore size and adsorption average pore width was calculated using the ratio of $4\ V/S_{BET}$; and, a pore size distribution between 1.70 and 3.00×10^2 nm in diameter was determined using the Barett, Joyner and Halenda (BJH) model equation. Micropores of less than 1.7 nm in diameter were not determined in this study.

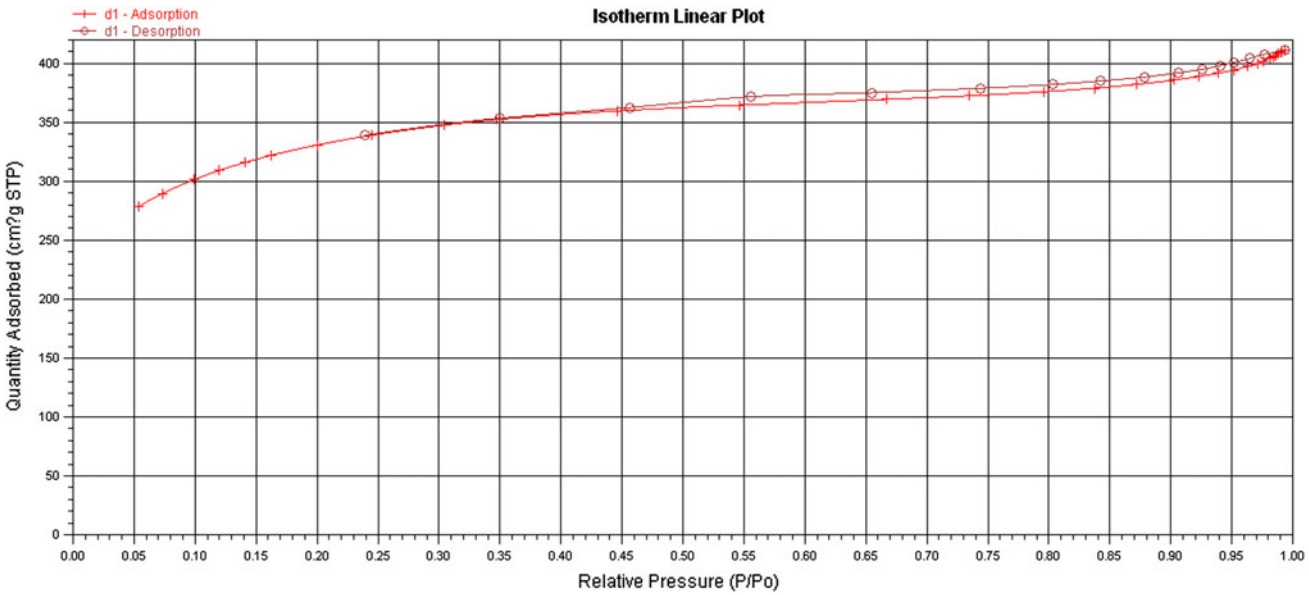

Fig. 1 Adsorption–desorption isotherms of N_2 at −196 °C on the AC prepared under the optimized conditions

Table 4 Pore structure parameters of activated carbon prepared under optimal conditions

S_{BET} (m^2 g^{-1})	V (cm^3 g^{-1})	V_{micro} (cm^3 g^{-1})	Microporosity (%)	W_d (nm)	S_{micro} (m^2 g^{-1})	S_{exter} (m^2 g^{-1})
1.12×10^3	0.636	0.160	25.2	2.27	486	634

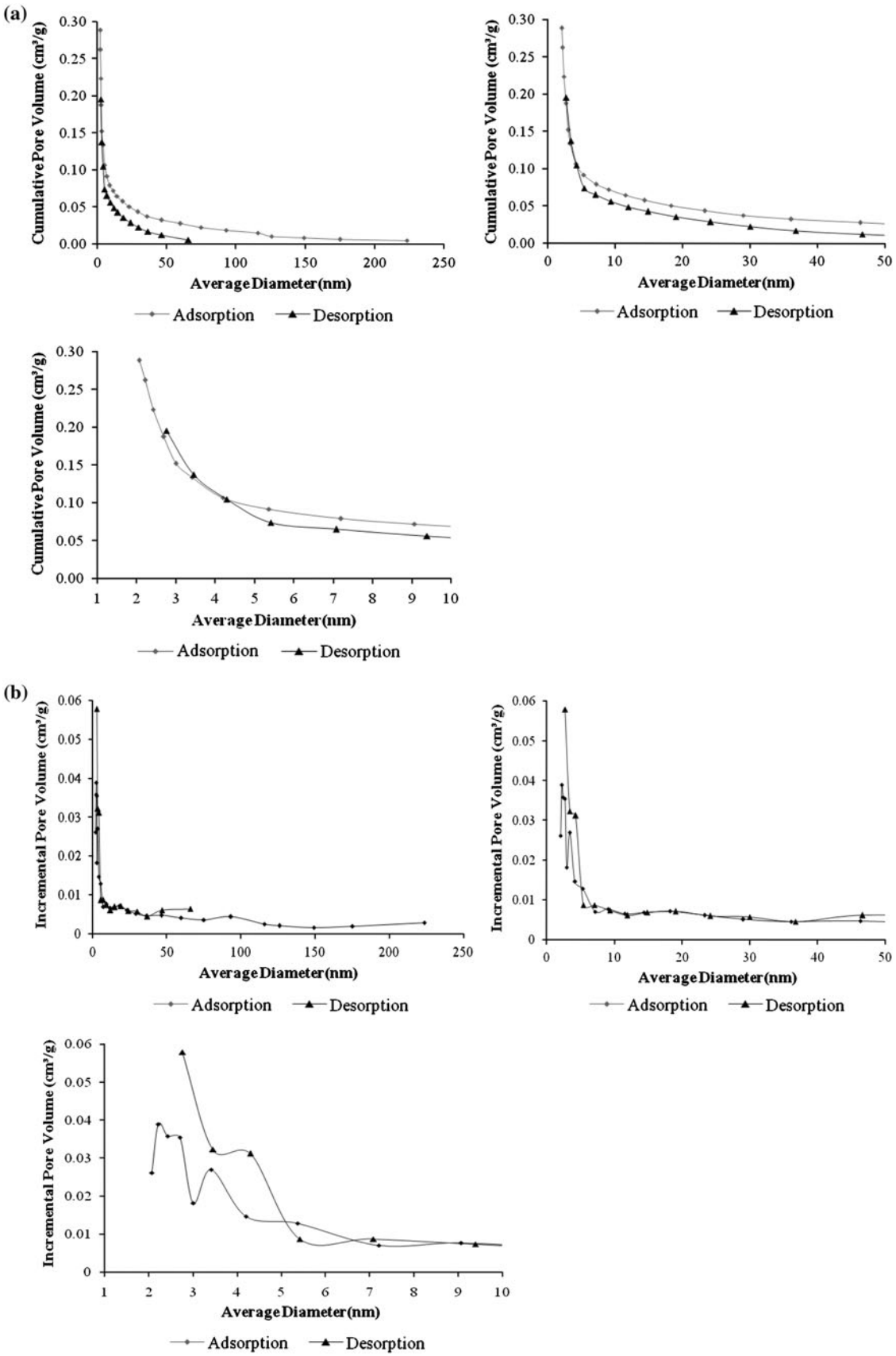
(a)
Cumulative Pore Volume (cm³/g)
Average Diameter(nm)
Adsorption
Desorption
(b)
Incremental Pore Volume (cm³/g)
Average Diameter(nm)
Adsorption
Desorption

◀ **Fig. 2** BJH pore size distribution of the AC prepared under the optimized conditions. **a** Cumulative pore volume curve, **b** incremental pore volumecurve, **c** pore size distribution curve

The morphology of the AC was examined by scanning electron microscopy (SEM) (Japan's Hitachi S-3400).

The functional groups on the surface of the activated carbon samples were identified by Fourier transform infrared (FTIR) spectroscopy. OMNIC software was used for data analysis.

3 Results and Discussion

3.1 Orthogonal Test Results

The results of L_9 (3^4) orthogonal array of designed experiments for the preparation of activated carbon and the yield, Iodine number and BET surface area of each prepared activated carbon sample are shown in Table 2. Analysis of the experimental results is shown in Table 3.

Iodine is considered as a molecular probe to assess the adsorption capacity of sorbents for solutes of molecular size less than 1 nm. Iodine number and BET surface area are normally listed as specification parameters for commercial ACs. Therefore, the AC yield (Y_1, %), Iodine number (Y_2, mg g^{-1}) and BET surface area (Y_3, m^2 g^{-1}) were determined. The k_n value is the average response value of the operational parameter at the level number n, with the optimum level value when k_n is a maximum. R is defined as the remainder of maximum subtract minimum of the same operational parameter k_n value. The magnitude of R reflects the influence of each factor on the corresponding response. The larger the R-value of a corresponding factor, the more significant the influence of that corresponding factor. From Table 3, there are significant differences in the yield, Iodine number and BET surface area of the activated carbons prepared under different conditions, with different factors having different influences on the prepared activated carbons. In this experiment, we designed nine tests. The Iodine number of the prepared activated carbon in five of the tests exceeded 500 mg g^{-1}, and a maximum Iodine number of 899 mg g^{-1} was achieved, while the yield was 13.3 % and BET surface area was 1.12×10^3 m^2 g^{-1}. The influence of each factor has the

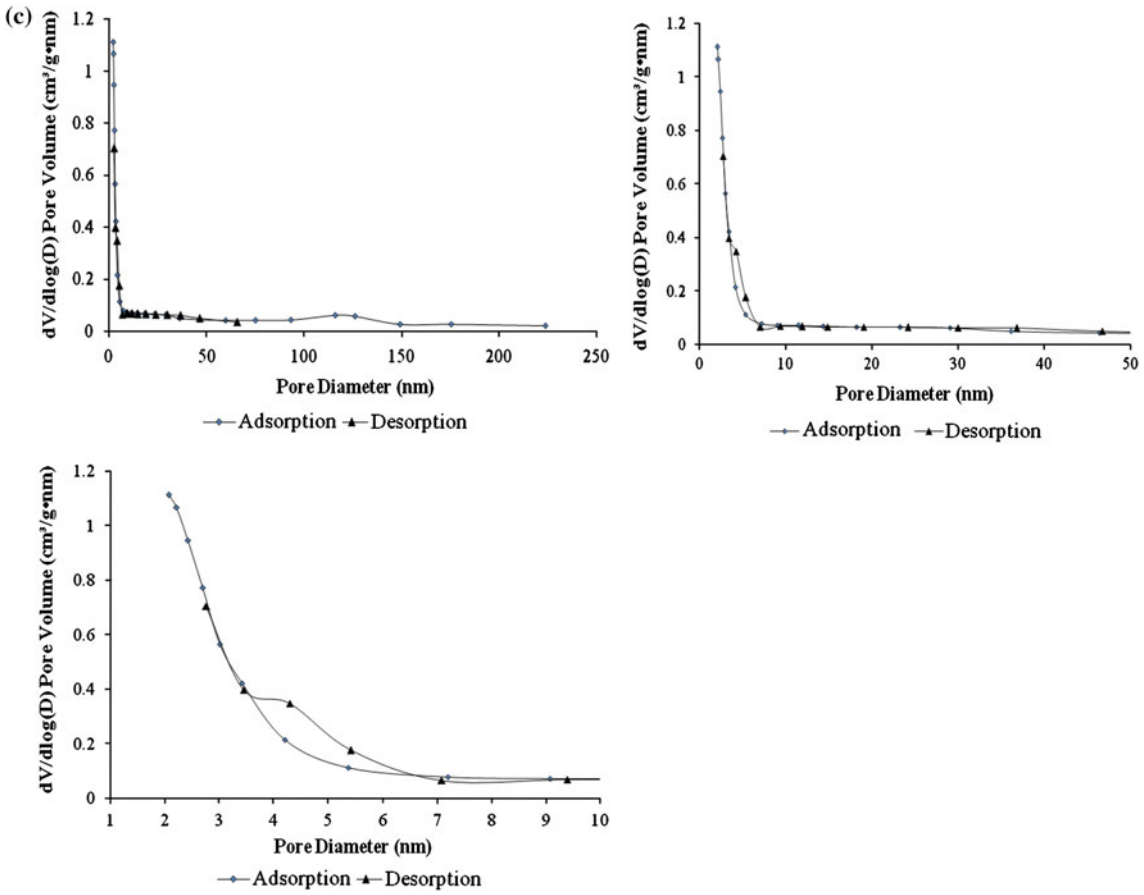

Fig. 2 continued

followings order: Iodine number $A_1 > B_1 > C_2$, BET surface area: $B_1 > A_1 > C_1$, yield: $C_1 > B_1 > A_3$. When optimizing these factors, the AC yield should also be taken into account, as production efficiency must be considered. With the experimental conditions described in Sect. 2.3, $A_1B_1C_1$ were determined as the optimal conditions for preparing activated carbon. The optimal weight ratio of NaOH to eucalyptus sawdust is 2:1, activation time is 30 min and activation temperature is 700 °C. Under optimized production conditions, the Iodine number of the prepared activated carbon is 899 mg g^{-1}, the BET surface area reaches 1.12×10^3 m^2 g^{-1}, and the yield of the AC is 13.3 %.

3.2 Pore Structure of the AC Prepared Under Optimal Conditions

The structural heterogeneity of AC plays an important role in the adsorption process, and numerous methods have been developed and applied to characterize this property. In this study, nitrogen adsorption–desorption isotherm and SEM methods were used to characterize the pore structure. FTIR techniques were also used to qualitatively characterize the functional groups on the optimized AC surfaces.

3.2.1 Nitrogen Adsorption–Desorption Isotherms

Nitrogen adsorption, because of the relatively small molecular diameter of nitrogen, is frequently used at −196 °C to probe porosity and surface area. It has become a standard procedure used to characterize porosity texture of carbonaceous adsorbents. The adsorption isotherm gives useful information about the porous structure of the adsorbent, heat of adsorption, and physical and chemical characteristics. Adsorption isotherms may be grouped into six types. Figure 1 illustrates the optimally prepared AC adsorption–desorption isotherms of N_2 at −196 °C. The AC exhibits type IV adsorption isotherms according to the International Union of Pure and Applied Chemistry (IUPAC) classification [20]. The step in the adsorption branch combined with the decline in the desorption branch is an indication of mesoporosity. This noticeable increase in the quantity adsorbed in the desorption branch can be attributed to capillary condensation and, since the P/P_0 position of the inflection point is related to the pore size, indicates good homogeneity of the sample and a fairly small pore size. The type IV isotherm is characteristic of solids having both microporous and mesoporous structures [20]. The initial part of the type IV isotherm follows the same path as the corresponding type II isotherm [21]. The initial part of the type II isotherm for carbon represents micropore fillings; and, the slope of the plateau at high relative pressures is attributed to the multilayer adsorption on the non-microporous surface; i.e., on the mesoporous, macroporous or on the external surfaces [22]. Thereafter, the isotherm of the AC prepared under optimal conditions can be mainly attributed to a monolayer–multilayer adsorption on the mesoporous walls [21].

3.2.2 Characterization of Pore Structure

The results for BET surface area (S_{BET}), micropore area (S_{micro}), external surface area (S_{exter}), single point adsorption total pore volume (V) of pores less than 284.8 nm in diameter at $P/P_0 = 0.993$, micropore volume (V_{micro}) and adsorption average pore width (W_d) (4 V/S_{BET}) obtained by applying the BET equation to N_2 adsorption at −196 °C are listed in Table 4.

Pore size distribution (PSD) is an important property for porous adsorbents. PSD determines the fraction of the total pore volume accessible to molecules of a given size and shape. According to IUPAC pore dimension classifications, the pores of a porous absorbent can be grouped into micropores ($d < 2$ nm), mesopores ($d = 2 - 50$ nm) and macropores ($d > 50$ nm). The average adsorption pore width (4 V/S_{BET}) of the AC prepared under optimal conditions was found to be 2.27 nm. The BJH adsorption and desorption cumulative surface areas (S_{BJH}) of pores between 1.70 and 3.00×10^2 nm in diameter were found to be 329 and 178 m^2 g^{-1}, respectively. The BJH adsorption and desorption cumulative volumes (V_{BJH}) of pores between 1.70 and 3.00×10^2 nm in diameter were found to be 0.289 and 0.196 cm^3 g^{-1}, respectively. The BJH adsorption and desorption average pore diameter ($4V_{BJH}/S_{BJH}$) of the AC samples were found to be 3.51 and 4.51 nm, respectively, indicating mesoporous absorbents. The pore size distribution calculated using the standard BJH method [23] is displayed in Fig. 2. The cumulative volume distribution (a) and the incremental volume distribution (b) show that a major part of the AC pore volume is distributed in pores with an average diameter of 2–100 nm; (c) shows that the AC is characterized by a single peak and has many wider mesopores (average pore diameter >10 nm). There are differences in all the results obtained from absorption and desorption data. In general, Fig. 2 shows that most of the AC pores are in the mesoporous range. The simultaneous presence of a microporous structure is indicated in Table 4. However, analysis of the total pore volume compare with the micropore volume shows a smaller contribution from the micropores (microporosity, 25.2 %). Thus, the prepared AC can be said to have both microporous and mesoporous structures; but, it is mainly mesoporous.

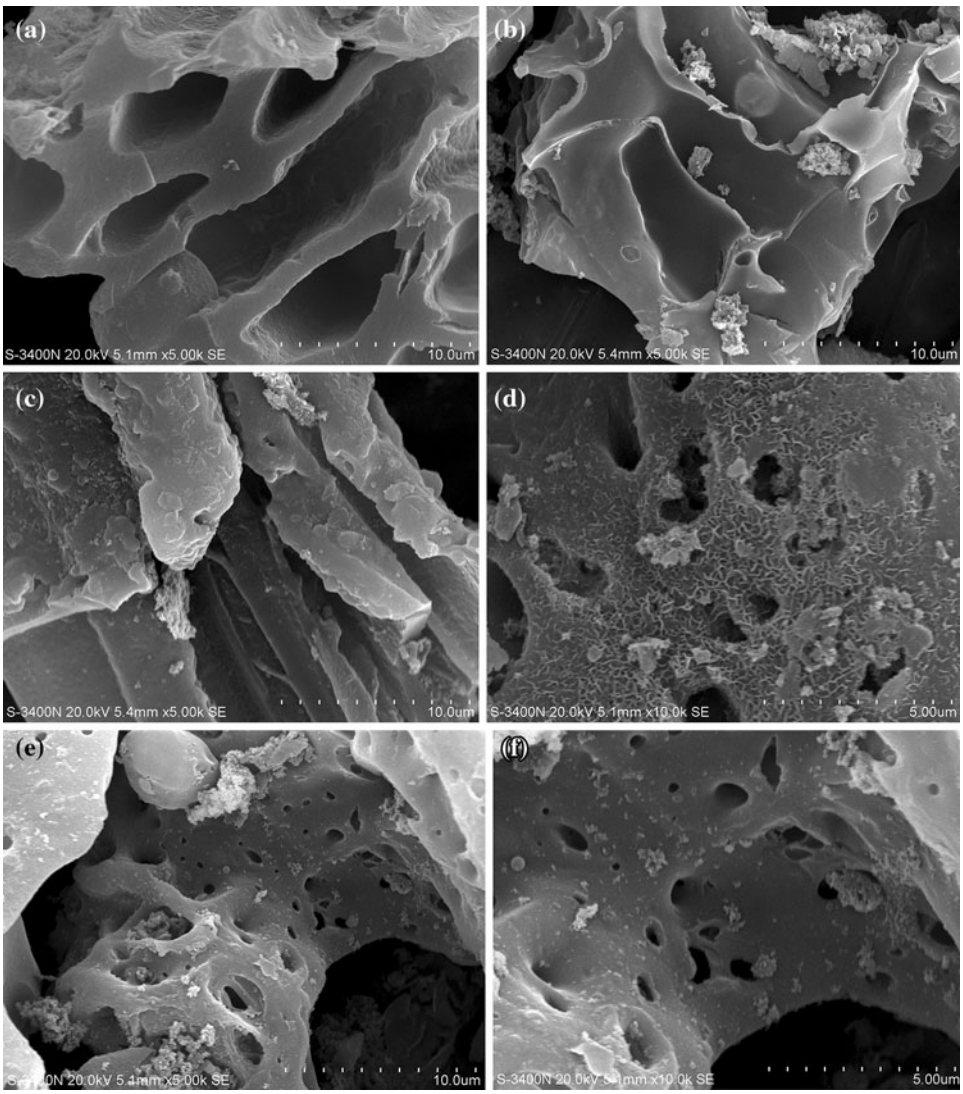

Fig. 3 SEM images of the AC prepared under the optimized conditions (**a**–**f**)

3.2.3 Surface Morphology

SEM was employed to observe the surface physical morphology of the AC. The SEM micrographs of the AC prepared under optimal conditions is shown in Fig. 3. The SEM images (a–c) (Fig. 3) show the development of capillary-like pore structures on the AC surface. Images (d–f) shows the external surfaces of the AC being full of irregular cavities as a result of activation. Those pores may be a result of the evaporation of the activation agent NaOH, decomposition of the eucalyptus sawdust, a chemical reaction between the carbonide and activation agent NaOH during activation, or the space previously occupied by the activation agent. From Fig. 3, there appears to be some particulate matter on the external surface of the activated carbon, which may be related to the activation agent. As mentioned above, the prepared AC mainly consists of mesopores; however, it also contains some micropores. It is clear that the prepared AC contains a redundant pore structure that is further supported by SEM.

3.3 FTIR Analysis of the AC Prepared Under Optimal Conditions

The FTIR spectra of the AC prepared under optimal conditions is shown in Fig. 4. It is noted that the absorption band at 3,431 cm^{-1} is due to the O–H stretching vibration. The emergence of the hydroxyl group may also indicate a certain relationship in water [24]. The band at 2,918 cm^{-1} is attributed to C–H ($–CH_2$, $–CH_3$, –CH=O) stretching vibrations [25]. The band at 1,639 cm^{-1} is attributed to the C=O stretching vibration and corresponds to carbonyl and carboxyl groups [26]. The band at 1,439 cm^{-1} is assigned to the scissoring vibration of the ($–CH_2$) group, which may overlap with the methyl group asymmetrical bending. It may also be attributed either to the in-plane bending of the H-bonded hydroxyl

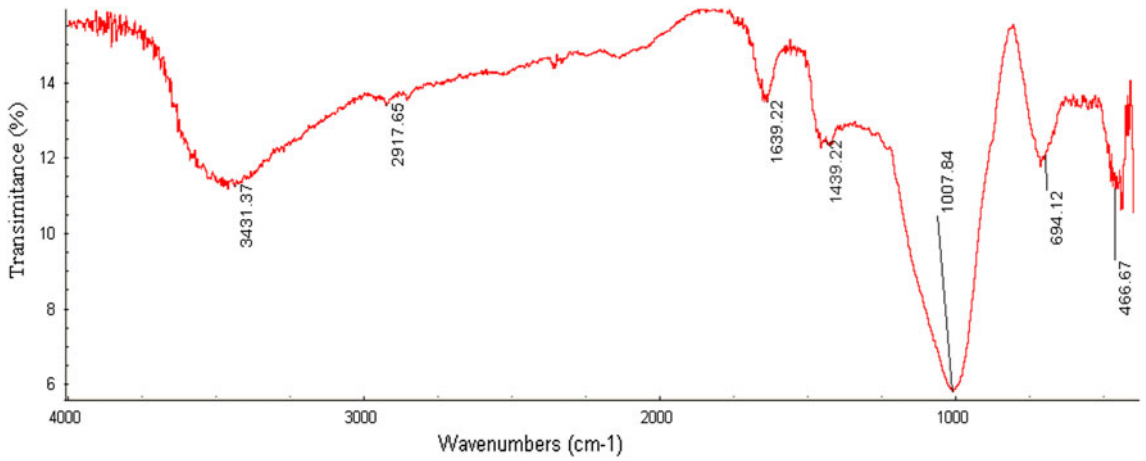

Fig. 4 FTIR spectra of AC based on eucalyptus sawdust prepared under optimized conditions

group, an O–H deformation vibration in carboxyl groups or a C–H bending vibration [25, 26]. The band at 1,007 cm^{-1} is associated with the aromatic C–H in-plane deformation, with symmetrical C–O stretching or C–O–C strong symmetrical bands [25]. The bands at 694 and 467 cm^{-1} are attributed to the –OH out-of-plane bending vibrations [25–29]. The surface functional groups of the AC are grouped into three types; carboxyl-type, carbonyl-type and hydroxyl-type [30]. The FTIR analysis indicates that hydroxyl or carbonyl compounds may exist on the surface of the prepared AC, although the results need to be verified by other methods, such as oxygen K-edge X-ray absorption near-edge structure spectroscopy to identify and quantify the surface functional groups on the carbon materials [30].

4 Conclusions

Waste eucalyptus sawdust can be used as a highly suitable raw material with NaOH used as an activation agent to prepare AC. When the eucalyptus sawdust mass was 30.00 g, with particle sizes between 0.25–0.42 mm, and the sawdust was heated and charred before activation by NaOH, the optimized conditions for the preparation of AC is as follows: mass ratio of NaOH to eucalyptus sawdust, 1:2; activation time, 30 min; and activation temperature, 700 °C. The Iodine number and BET surface area of the produced activated carbon was 899 and 1.12×10^3 $m^2\ g^{-1}$, respectively, with a 13.3 % yield. The AC is mainly mesoporous.

Acknowledgments The authors are grateful for support from the National Natural Science Foundation of China (No. 21266002). This project was also supported by Guangxi University and Guangxi Education Department Education Reform in the 21st Century Research Fund of China (No. 2011JGA010), the Dean Project of Guangxi Key Laboratory of Petrochemical Resource Processing and Process Intensification Technology of China (No. 11-C-01-01), the Scientific Research Foundation of Guangxi University (No. XBZ110639) and 2012–2013 "college students' innovative entrepreneurial training plan" Guangxi autonomous region level Innovation training project (No. 61).

References

1. Y. Chen, Y.C. Zhu, Z.C. Wang, Y. Li, L.L. Wang, L.L. Ding, X.Y. Gao, Y.J. Ma, Y.P. Guo, Adv. Colloid Interfac. **163**, 39 (2011)
2. J.M. Dias, M.C.M. Alvim-Ferraz, M.F. Almeida, J. Rivera-Utrilla, M. Snachez-polo, J. Environ. Manage. **85**, 833 (2007)
3. K.L. Gu, Chem. Ind. Forest Prod. **3**, 37 (1999)
4. J. Rivera-Utrilla, M. Sanchez-Polo, V. Gomez-Serrano, P.M. Alvarez, M.C.M. Alvim-Ferraz, J.M. Dias, J. Hazard. Mater. **187**, 1 (2011)
5. O. Ioannidou, A. Zabaniotou, Renew. Sust. Energ. Rev. **11**, 1966 (2007)
6. M.K.B. Gratuito, T. Panyathanmaporn, R.A. Chumnanklang, N. Sirinuntawittaya, A. Dutta, Bioresource Technol. **99**, 4887 (2008)
7. A.H. Basta, V. Fierro, H. El-Saied, A. Celzard, Bioresource Technol. **100**, 3941 (2009)
8. J. Hayashi, T. Horikawa, K. Muroyama, V.G. Gomes, Micropor Mesopor Mat. **55**, 63 (2002)
9. R.L. Tseng, J. Hazard. Mater. **147**, 1020 (2007)
10. C. Saka, J. Anal. Appl. Pyrolysis **95**, 21 (2012)
11. T. Budinova, E. Ekinci, F. Yardim, A. Grimm, E. Bjornbom, V. Minkova, M. Goranova, Fuel Processing Technol. **87**, 899 (2006)
12. S. Aber, A. Khataee, M. Sheydaei, Bioresource Technol. **100**, 6586 (2009)
13. H. Deng, L. Yang, G. Tao, J. Dai, J. Hazard. Mater. **166**, 1514 (2009)
14. I. Kula, M. Ugurlu, H. Karaoglu, A. Celik, Bioresource Technol. **99**, 492 (2008)
15. N.C. Tancredi, T. Cordero, J. Rodriguez-Mirasol, J.J. Rodriguez, Fuel **75**, 1701 (1996)
16. A.M.M. Vargas, A.L. Cazetta, C.A. Garcia, J.C.G. Moraes, E.M. Nogami, E. Lenzi, W.F. Costa, V.C. Almeida, J. Environ. Manage. **92**, 178 (2011)
17. R.L. Tseng, J. Colloid Interf. Sci. **303**, 494 (2006)

18. Y.B. Tang, Q. Liu, F.Y. Chen, Chem. Eng. J. **203**, 19 (2012)
19. H. Deng, G.L. Zhang, X.L. Xu, G.H. Tao, J.L. Dai, J. Hazard. Mater. **182**, 217 (2010)
20. K.W. Sing, D.H. Everet, R.A.W. Haul, L. Moscou, R.A. Pierotti, J. Rouquero, T. Siemieniewasa, J. Pure Appl, Chem. **57**, 603 (1985)
21. Z. Ryu, J. Zheng, M. Wang, B. Zhang, Carbon **37**, 1257 (1999)
22. F. Rouquerol, J. Rouquerol, K.S.W. Sing, *Adsorption by powders and porous solids. Principles, methods and application* (Academic Press, San Diego, 1999), pp. 19–20
23. P.E.P. Barrett, L.G. Joyner, P.P. Halenda, J. Am. Chem. Soc. **73**, 373 (1951)
24. Y.Y. Guo, D.A. Rockstraw, Micropor. Mesopor. Mat. **100**, 12 (2007)
25. A.H. El-Sheikh, A.P. Newman, H.K. Al-Daffaee, S. Phull, N. Cresswell, J. Anal. Appl. Pyrolysis **71**, 151 (2004)
26. C. Moreno-Castilla, M.V. Lopez-Ramon, F. Carrasco-Marin, Carbon **38**, 1995 (2000)
27. J.J. Chen, Y.B. Zhai, H.M. Chen, C.T. Li, G.M. Zeng, D.X. Pang, P. Lu, Appl. Surf. Sci. **263**, 247 (2012)
28. K.Y. Foo, B.H. Hameed, Chem. Eng. J. **187**, 53 (2012)
29. K.Y. Foo, B.H. Hameed, Bioresource Technol. **112**, 143 (2012)
30. K.S. Kim, P.Y. Zhu, N. Li, X.L. Ma, Y.S. Chen, Carbon **49**, 1745 (2011)